JACS
JOURNAL OF THE AMERICAN CHEMICAL SOCIETY
Article
pubs.acs.org/JACS

Single-Dot Spectroscopy of Zinc-Blende CdSe/CdS Core/Shell Nanocrystals: Nonblinking and Correlation with Ensemble Measurements

Haiyan Qin,*[,†,§] Yuan Niu,[†,§] Renyang Meng,[†] Xing Lin,[‡] Runchen Lai,[†] Wei Fang,*[,‡] and Xiaogang Peng*[,†]

[†]Center for Chemistry of Novel and High-Performance Materials, and Department of Chemistry, Zhejiang University, Hangzhou, 310027, P. R. China

[‡]State Key Laboratory of Modern Optical Instrumentation, Department of Optical Engineering, Zhejiang University, Hangzhou, 310027, P. R. China

Supporting Information

ABSTRACT: Here we report the first series of phase-pure zinc-blende CdSe/CdS core/shell quantum dots (QDs) with reproducibly controlled shell thickness (4−16 monolayers), which are nonblinking (≥95% 'on' time) in single-exciton regime for the entire series. These unique QDs possess well-controlled yet simple excited-state decay dynamics at both single-dot and ensemble levels, extremely small nonblinking volume threshold, if any, and unique 'on' and 'off' probability statistics. The outstanding optical properties of the QDs at the single-dot level were found to be correlated well with their ensemble properties. These small and bright nonblinking QDs offer promising technical application prospect in both single-dot and ensemble levels. The consistent and reproducible experimental results shed new light on the mechanisms of blinking of QDs.

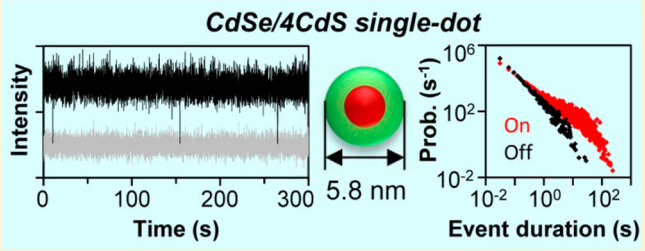

INTRODUCTION

Colloidal semiconductor nanocrystals (quantum dots, QDs) have been actively pursued as a new generation of luminescence materials because of their tunable, narrow-band, and bright luminescence.[1] Photoluminescence (PL) blinking of single QD—the PL intensity of single QD randomly switching between 'on' and 'off' under continuous excitation—is a puzzling phenomenon.[2] Blinking casted significant doubts on applications of QDs in fields requiring continuous excitation and emission, such as light-emitting diodes,[3] single-molecular tracking,[4] and single-photon sources.[5] Fundamentally, poor understanding of QDs blinking sets a roadblock for establishment of single-dot spectroscopy[6−11] as well as correlation of optical properties at single-dot and ensemble levels. At present, a huge number of QD systems with various compositions have been reported to be of high PL quantum yield (QY), but only several special QD systems were found to be nonblinking.[12−16] Furthermore, for those nonblinking systems, another level of inconsistency exists in literature, that is, the irreproducibility of the experimental results. Such inconsistency is common even with the most established wurtzite (hexagonal) CdSe/CdS core/shell QDs with extremely thick CdS shell (>15 monolayers of CdS shell).[14,15,17,18] For instance, a nonblinking volume threshold per dot for wurtzite CdSe/CdS core/shell QDs were recently reported to be 750 nm^3 by Ghosh et al.[17] and 390 nm^3 by Chen et al.[18]

Inconsistency between single-dot and ensemble optical properties of the same batch of QDs could be caused by different reasons. The first reason is the inhomogeneity of the QDs samples, especially that of trap states accessible to QDs under excitation. In principle, all luminescence processes, including QDs-related ones, depend on excited-state properties. However, synthesis of QDs has been often focused on control of their size and shape,[19,20] with less concerns of their optical properties through synthetic control. Specifically, PL decay dynamics of a given type of QDs reported in literature generally varied significantly at an ensemble level and was often found to be quite complex, i.e., with multiple decay channels instead of single-channel decay. At the single-dot level, if one observed a single dot for a given period of time, the PL decay lifetime was often observed to fluctuate substantially.[9,21−25] Furthermore, PL decay dynamics was generally found to vary substantially from one dot to another in a given sample.[9,21,24]

The second possible cause of the inconsistency might come from the different measurement scheme. Nearly all ensemble measurements are performed within the single-exciton regime by tuning the excitation power in the low part of the linear optical window. However, because of the quite low signal-to-noise ratio and relatively low PL QY, single-dot measurements might be performed with relatively high excitation power,

Received: July 30, 2013
Published: December 17, 2013

ACS Publications © 2013 American Chemical Society

dx.doi.org/10.1021/ja4078528 | J. Am. Chem. Soc. 2014, 136, 179−187

which could easily get into multiexciton regime. The fluctuation of PL decay lifetime at a single-dot level[9,21−25] mentioned above further complicates the situation by making it difficult to account the excitation power level reliably.

Phase-pure zinc-blende (face-centered cubic) CdSe/CdS core/shell QDs were reported to be synthesized with well-controlled and reproducible PL decay dynamics when their CdS shell thickness was up to 4 monolayers.[26] This series of high-quality QDs has been further extended to up 16 monolayers of CdS shell (to be published separately). These phase-pure core/shell QDs possessed unique single-channel PL decay dynamics when the CdS shell thickness was roughly between 3 and 8 monolayers of CdS. According to theory,[27] zinc-blende QDs should have less complex energy levels than their wurtzite counterparts at the excited state due to a more symmetric crystal field of the zinc-blende structure, which could thus demonstrate well-controlled and simple PL decay dynamics. Furthermore, excellent and reproducible optical properties of this new series of phase-pure zinc-blende core/shell dos at ensemble level—PL peak width ∼80 meV for all samples in the series and PL QY up to >90%—were found to be substantially better in comparison to their wurtzite counterparts.[26] To our knowledge, single-dot spectroscopic studies with such a series of high-quality QDs have not yet been reported even for the mostly studied wurtzite CdSe/CdS core/shell QDs. With these facts, we thus anticipated that such a series of QDs might offer unique opportunities for obtaining consistent results at single-dot level to correlate with their ensemble optical properties. In addition, these samples should further illustrate unique shell-thickness-dependent optical properties at single-dot level, given their outstanding structural/optical quality at the ensemble level across the entire series.

Experimental results to be discussed below shall illustrate that the entire series of QDs, including those QDs with 4−6 monolayers of CdS shells with the total volume being as small as 100 nm^3 per dot, were found to be nonblinking. Consistent with the hypothesis mentioned above, high structural/optical quality of QDs coupled with judicious experimental design in single-dot spectroscopy with their PL decay lifetime as guidelines could offer consistent and reproducible results for single-dot spectroscopy. Furthermore, the single-dot results to be described below were found to correlate well with those from ensemble measurements.

RESULTS AND DISCUSSIONS

Sample Information and Experimental Design. Phase-pure zinc-blende CdSe/CdS core/shell QDs[26] with quantitatively reproducible shell thicknesses up to 16 monolayers of CdS were studied (Figure 1). For simplicity, CdSe/CdS core/shell QDs with x monolayers of CdS shell might be written as 'CdSe/xCdS' below. The QDs with 4−6 monolayers of CdS, 7−11 monolayers of CdS, 12−16 monolayers of CdS, and >16 monolayers of CdS would be regarded as thin shell, medium shell, thick shell, and extremely thick shell (or giant) ones, respectively. The QDs with 1−3 monolayers of CdS shell were approaching detection limit for the systematic studies presented here and thus would not be discussed.

To ensure single-dot measurements in single-exciton domain, the average number of photons absorbed for a QD within one single-exciton lifetime period was kept under 0.01 (see Supporting Information for detailed calculations). This limit was established using a general guideline used in ensemble

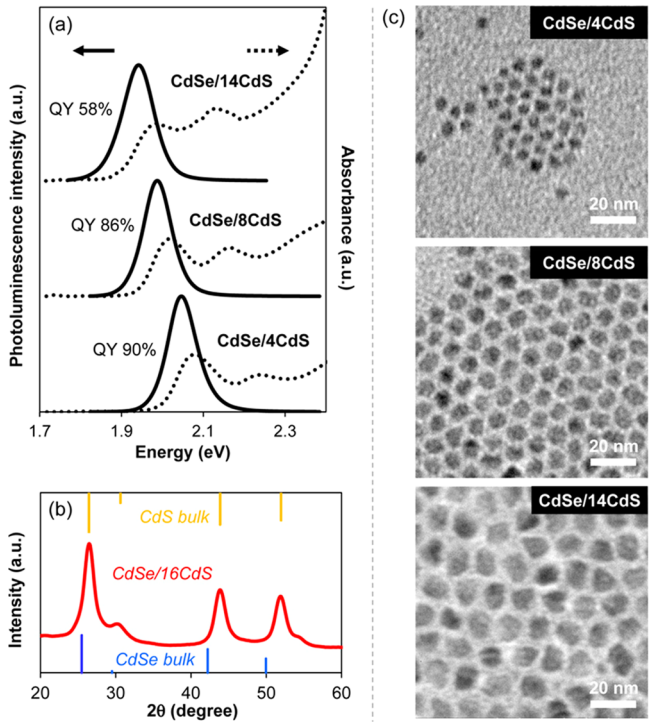

Figure 1. (a) Evolution of UV−vis and PL spectra of ensemble zinc-blende CdSe/CdS core/shell QDs upon shell growth. The absolute PL QY values of ensemble samples were stated. (b) X-ray powder diffraction pattern of zinc-blende CdSe/CdS core/shell QDs with 16 monolayers of shell. Blue and yellow lines indicate the standard peak positions of bulk zinc-blende CdSe and CdS, respectively. (c) TEM images of zinc-blende CdSe/CdS core/shell QDs with 4, 8, and 14 monolayers of shell.

measurements[28] and shall be confirmed by the experimental results below. The up limit of excitation power with a continuous laser at 405 nm was calculated to be in the range between 0.3 and 1.5 W/cm^2 for the QDs with different CdS shell thicknesses, which was found to be in the similar excitation power range used previously for the wurtzite counterparts in literature.[18] The power variations between samples with different shell thicknesses were a result of assuming the CdS shell contributing most absorption cross-section at 405 nm in a core/shell dot. All optical measurements were performed under ambient conditions (21 ± 3 °C and <40% of relative humidity). It should be mentioned that the spectroscopic properties of ensemble QDs were identical with 405 and 515 nm excitation (see Figure S1). Moreover, the spectroscopic properties of single QDs excited with a pulsed laser were identical to those with a continuous-wave laser (compare Figure S2 with Figure 2a), as long as the average number of photons absorbed for a dot within one pulse kept under a similar level.

Ensemble Optical and Structural Properties of the CdSe/CdS Core/Shell QDs. The series of core/shell QDs were synthesized using a scheme newly developed on the basis of a recent report.[26] In comparison to the literature report,[26] this new scheme made it possible to synthesize the core/shell nanocrystals with much improved optical properties, even for the thin-shell dots (Figure 1). Along with the growth of CdS shell, the absorption and PL spectra both shifted substantially and continuously to lower energy (Figure 1a). This suggests epitaxial growth of CdS shell outside the CdSe core, instead of

dx.doi.org/10.1021/ja4078528 | J. Am. Chem. Soc. 2014, 136, 179−187

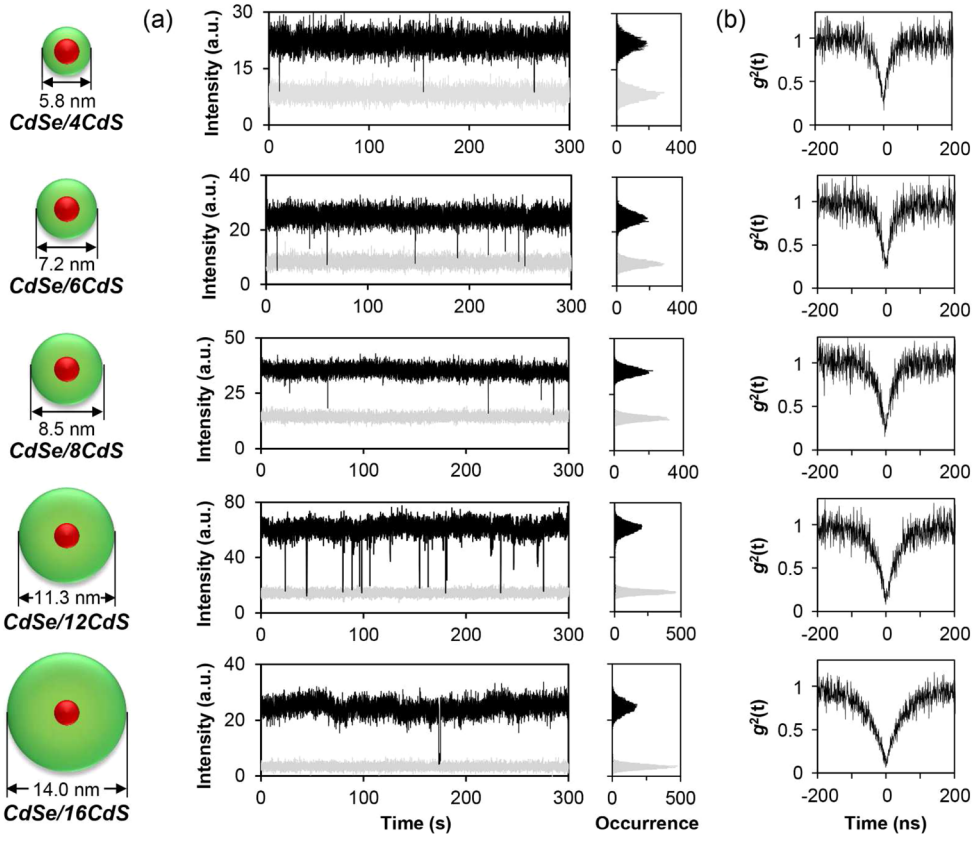

Figure 2. Blinking behavior of single CdSe/CdS QDs and their antibunching curves. (a) Representative PL intensity time traces of single zinc-blende CdSe/CdS core/shell QDs (black traces) with core radius of 1.55 nm and shell thickness varied from 1.36 to 5.44 nm, corresponding to 4−16 monolayers of CdS shell. The data were recorded by an EMCCD with offset correction. The binning time is 30 ms. The gray traces are the corrected background noise intensities. Histograms to right indicate the distribution of intensities observed in the traces. (b) Antibunching curves of the single QDs in (a). The data were recorded by a single-photon counting system with two avalanche photodiodes.

alloying. The full width of half-maximums (fwhms) of their emission peaks were quite narrow, especially for the thin-shell ones (~80 meV). The PL QY of the ensemble samples increased to ~90% for the thin-shell QDs and gradually dropped to ~50% for thick-shell ones.

XRD pattern of the CdSe/CdS QDs with 16 monolayers of shell shown in Figure 1b is consistent with the zinc-blende crystal structure without minor wurtzite diffraction signature. This indicates that the zinc-blende crystal structure was retained along the whole shell growth process of up to 16 monolayers of shell. TEM measurements in Figure 1c revealed that the phase-pure zinc-blende CdSe/CdS QDs with different shell thicknesses were all nearly spherical in shape and had good size and shape distribution. This agreed with their narrow and symmetric PL spectra in Figure 1a.

Entire Series Nonblinking in Single-Exciton Regime. Experimental results (Figure 2a and Supporting Information Movies) recorded by a fluorescence microscopic system with an EMCCD revealed that, within targeted single-exciton regime, zinc-blende CdSe/CdS core/shell QDs with 4−16 monolayers of CdS shell were all nearly nonblinking at single-dot level. To our knowledge, this represents the first series of nonblinking core/shell nanocrystals covering such a broad range of shell thickness, and the QDs within thin-shell regime are likely the smallest nonblinking CdSe/CdS core/shell QDs discovered so far. In addition, these nonblinking QDs, especially those thin-shell ones, are substantially smaller than those nonblinking 'giant QDs' which were defined as wurtzite CdSe/CdS core/shell QDs with 16−22 monolayers of CdS.[14,15,17]

Second-order photon correlation (or antibunching) experiments performed with a time-correlated single-photon counting system were carried out to confirm that all measurements were associated with a single dot.[29,30] In all curves in Figure 2b for samples with different CdS shell thicknesses, the $g^2(0)$—the value of normalized second-order correlation function ($g^2(t)$) at time (t) being 0 in each curve—was significantly smaller than 0.5. This indicates that the measured emission light source is a single and anharmonic quantum emitter, implying a single QD in our case.[29,30] The $g^2(0)$ values did not reach zero likely due to background noise and possibly a very small amount of multiexciton emission. In principle, dots with thick CdS shell should be easier to generate multiexciton emission due to their relatively larger absorption cross sections. Thus, given the reduced values of $g^2(0)$ for thick-shell dots in Figure 2b, the small $g^2(0)$ values—between 0.1 and 0.2 in Figure 2b—should be most likely associated with background noise. The contribution of background noise could come from two pathways, i.e., correlation between background photons as well as correlation between a background photon and a dot PL photon.

The antibunching curves could be applied for examining whether the single-dot measurements using the continuous wave laser was within single-exciton regime by studying the PL decay lifetime. Ideally, $g^2(t)$ function form should have the same channel number as the time-resolved PL decay curve.

dx.doi.org/10.1021/ja4078528 | J. Am. Chem. Soc. 2014, 136, 179−187

However, due to the relatively poor signal-to-noise ratio, we only fitted the normalized second-order correlation function with first approximation, $g^2(t) = 1 - a\cdot\exp(-t/\tau)$,[29,30] where τ is the average PL decay lifetime and a is a constant. The fitting results in Table 1 revealed that the average PL decay lifetime

Table 1. Representative PL Decay Lifetimes Obtained at Single-Dot and Ensemble Levels

	Single-dot level, antibunching	Single-dot level, PL decay curves			Ensemble level, PL decay curves		
	τ (ns)	τ_1 (ns)	τ_2 (ns)	$\bar{\tau}$ (ns)	τ_1 (ns)	τ_2 (ns)	$\bar{\tau}$ (ns)
CdSe/4CdS	20.2	19.0	–	19.0	17.4	–	17.4
CdSe/8CdS	26.2	20.7	35.6	27.6	19.9	31.0	23.4
CdSe/12CdS	35.1	28.6	44.3	35.6	25.8	44.8	33.0
CdSe/16CdS	47.7	31.0	59.7	52.1	32.7	68.6	45.4

*$\bar{\tau}$ was calculated by accounting the contributions of all channels found in a specific measurement of PL decay curves for both single-dot and ensemble levels. For a double-channel decay, it is given by $\bar{\tau} = f_1\tau_1 + f_2\tau_2$, where f_1 and f_2 are the fractional contributions of two channels. (See more details in Supporting Information and Table S1). All lifetime values in single-dot level were average values over many single dots.

values obtained in this way were all consistent with the ensemble values. This implies that the original intention—measuring single-dot spectroscopic properties in single-exciton regime—was likely realized. This is so because the PL decay lifetime in multiexciton regime was known to be significantly shorter than the corresponding single-exciton value.[31]

Consistent Excited-State Decay Dynamics at Single-Dot and Ensemble Levels. While the average lifetime values obtained by fitting the antibunching curves could help to verify measurements within single-exciton regime, it could not offer any information on PL decay lifetime fluctuation observed commonly in single-dot measurements.[9,21,22] Furthermore, it does not provide information on the number of PL decay channels and contribution of each channel, which are needed for correlating excited state properties at single-dot and ensemble levels. All these must be provided by transient PL measurements using a pulsed laser.

The PL decay curves in Figures 3 and S3 obtained using a pulsed laser for the thin-shell QDs at both ensemble and single-dot levels could be well fitted by a single-exponential decay function with a goodness-of-fit χ_R^2 <1.30 (see full data series in Table S1). With medium-shell QDs as a transition, PL decay dynamics gradually evolved into double-channel PL decay for both single-dot and ensemble measurements (Figure 3 and Table 1). It is notable that the PL decay dynamics for ensemble QDs was identical with excitation wavelengths being 405 and 515 nm (Figure S1). This implies that the PL decay dynamics is insensitive to excitation of either the core (by 515 nm laser) or mainly the shell (by 405 nm laser). This should be due to the fast (a few picoseconds) carrier relaxation from shell to core,[32] orders of magnitude faster than the time resolution of experimental system as well as the exciton lifetime. For a similar reason, all we could observe in the experiments (e.g., PL time traces, antibunching traces, and transient PL decay curves) only reflected the carrier dynamics that took place in the core, which would exclude the differences caused by using either 515 or 405 nm laser as the excitation. The appearance of the second channel could be a result of delocalization of electron wave function into the thick CdS shell as suggested in literature for wurtzite CdSe/CdS core/shell QDs.[33]

It should be noticed that the peak photon counts for the ensemble PL decay experiments were set to 5000 for accurate measurements at a high signal-to-noise ratio. Despite the noise level was much lower with avalanche photo diode as detector compared to EMCCD, the signal-to-noise ratio for the single-dot PL decay experiments was still limited by the low signal level and poor collection efficiency. Although the peak photon counts were 5000 or more for single-dot experiments, a good portion of them were inevitably background photons. The high noise level in single-dot PL decay measurements would lead to relatively large deviation of the lifetime value of the long lifetime component. In any case, the good correlation of number of channels and lifetime value(s) for each channel in single-dot and ensemble measurements is evidenced in Figure 3 and Table 1.

Ghosh et al. suggested that 65 ns was the nonblinking threshold of PL decay lifetime for CdSe/CdS core/shell nanocrystals,[17] and this threshold was lowered to ~32 ns by Chen et al. recently.[18] Evidently, all lifetime values (being the average lifetime for double-channel ones) of the zinc-blende nonblinking QDs were in the range between 19 and 52 ns in Figure 3 and Table 1.

Several types of inhomogeneity/inconsistency of the PL decay dynamics of single dots within a QD sample have been reported by different research groups.[9,21,23−25] The first type was temporal fluctuation of PL decay lifetime for a give dot.[21,23−25] The second type was the number of PL decay channels varied dramatically from dot to dot within one

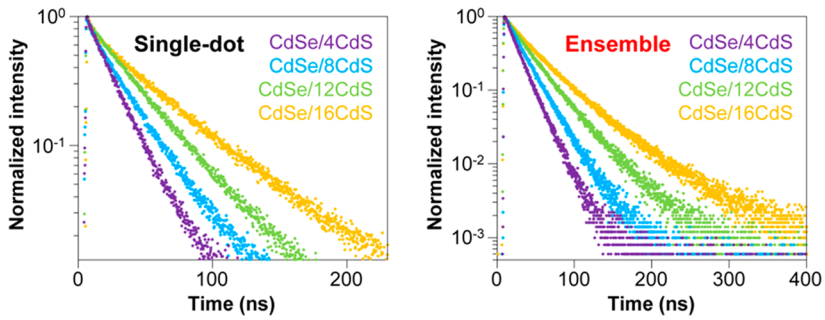

Figure 3. Representative transient PL decays of single (left panel) and ensemble (right panel) zinc-blende CdSe/CdS core/shell QDs with different shell thicknesses.

dx.doi.org/10.1021/ja4078528 | J. Am. Chem. Soc. 2014, 136, 179−187

sample.[9] The third type was the average lifetime changed widely from dot to dot, with fwhm of lifetime value distribution reported to be up to tens of nanoseconds.[24] As shown in Figure 4a,b, there was no apparent temporal fluctuation of PL decay

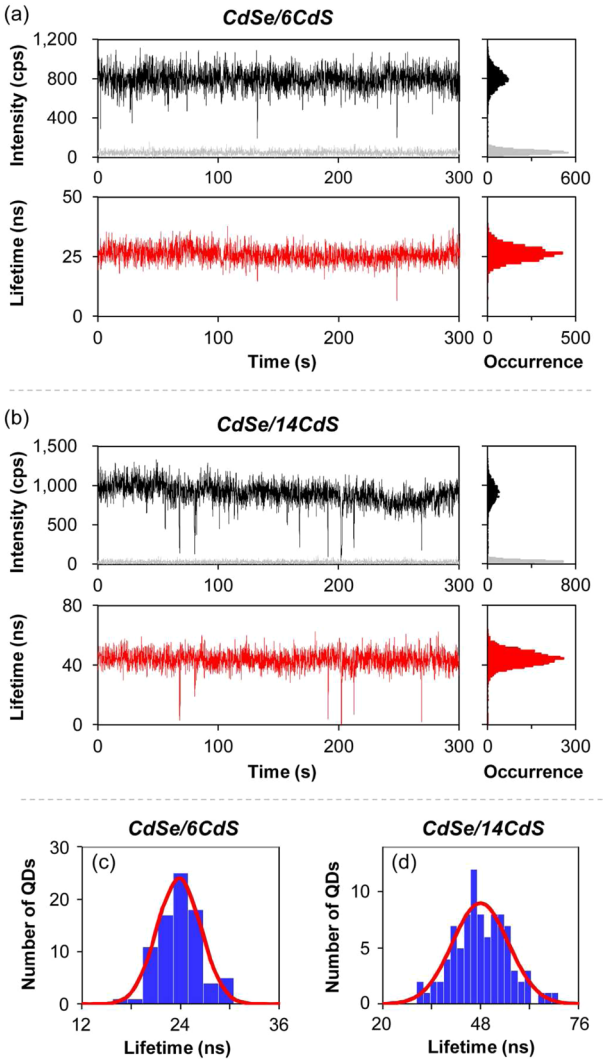

Figure 4. Homogeneity and consistency of the PL decay dynamics of single dots. (a) and (b) Representative PL intensity (black traces) and lifetime time traces (red traces) of single zinc-blende CdSe/CdS core/shell QDs with (a) 6 and (b) 14 monolayers of CdS shell. The PL intensity and corresponding lifetime time traces were recorded simultaneously by a single-photon counting system with an avalanche photodiode. The gray traces are the background noise intensities. Histograms to right indicate the distribution of intensities and lifetimes observed in the traces. (c) and (d) PL decay lifetime statistics (blue columns) of single zinc-blende CdSe/CdS core/shell QDs with 6 (b, 82 single dots) and 14 (c, 91 single dots) monolayers of CdS shell. The red curves indicate a Gaussian fit.

lifetime at single-dot level with either thin- or thick-shell dots during the observation period of 5 min. The PL decay dynamics also hold favorable consistency from dot to dot in the same sample. Despite of normalized distribution for the PL decay lifetime of a large quantity of QDs, number of decay channels remained the same (Figures 4c,d and S4). Quantitatively, all curves for CdSe/6CdS single dots could be well fitted into a single-exponential decay function with very similar lifetime values (fwhm being ~6 ns). Conversely, the average lifetime values of CdSe/14CdS single dots, fitted with a double-exponential decay function, had a wider distribution (fwhm being ~19 ns), which was likely due to the less spherical and nonuniform shape of the dots in the thick-shell regime (Figure 1c).

Overall, great correlation for the PL decay results between single-dot and ensemble levels are evidenced in Figure 3 and Table 1 across the entire series of QDs. Results in Figure 3 first supported the conclusion, drawn with the antibunching measurements using continuous laser (see above), that the single-dot PL intensity time traces (Figures 2 and S2) were all in the single-exciton regime. Second, they verified the high optical homogeneity of the QDs within a sample, especially the elimination of trap states accessible to the excited state. This should be true at least for those samples with single-exponential PL decay—the QDs with <8 monolayers of CdS shell in the series. Third, the PL decay dynamics of the thin- and medium-shell dots in this unique series of phase-pure QDs was likely approaching the intrinsic pathway(s) of the system at both single-dot and ensemble levels.

Transition from Binary Nonblinking to Nonbinary Nonblinking. Meijerink et al. predicted that QDs with single-exponential PL decay dynamics at an ensemble level would be ideal QDs with a series of unique properties.[34] This is so, as discussed above, because QDs with single-exponential decay dynamics mean that their excited-state properties are homogeneous, i.e., only emitting with a single and fixed channel. Consequently, the emission would not only be efficient at the ensemble level but also show a constant and nonblinking intensity at the single-dot level. Such a special type of nonblinking is known as '0−1' binary nonblinking. To our knowledge, this has not yet been fully verified by experiments. In terms of applications, such '0−1' nonblinking QDs with stable emission intensity should be of interest for single molecular tracking and single-photon sources.

Quantitatively, the intrinsic intensity bandwidth of a given PL intensity histogram (Figure 2a) could be calculated from the PL signal to background intensity ratio and the bandwidth of the background (see Supporting Information for calculation details). Evidently, the intrinsic intensity bandwidth for the PL intensity histograms in Figure 2a with single-channel decay was found to be consistent with '0−1' nonblinking behavior. To further confirm this unique nonblinking feature, multiple dots (~50 per sample) were measured and calculated for each sample. The results in Figure 5 suggest that such '0−1' nonblinking behavior was a common feature across each sample with single-channel PL decay dynamics. Consistent with the

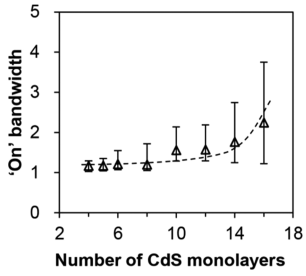

Figure 5. Average relative 'on' state intensity bandwidth for single zinc-blende CdSe/CdS core/shell QDs with different number of CdS shell monolayers. More than 50 dots are randomly selected and measured for each QD sample.

dx.doi.org/10.1021/ja4078528 | J. Am. Chem. Soc. 2014, 136, 179−187

gradual appearance of the second emissive channel for thick-shell QDs (see Figure 3 and the related text), the 'on' state intensity bandwidth increased as the shell thickness increased (Figure 5). The gradual increase of the 'on' bandwidth for the medium- and thick-shell dots in Figure 5, indicating nonbinary blinking, was found to be consistent with the gradual appearance of the second channel for corresponding samples (see Figure 3 and the related text).

Is There a Nonblinking Volume Threshold for Zinc-Blende CdSe/CdS Core/Shell QDs? Different from their zinc-blende counterparts discussed in this report, wurtzite CdSe/CdS core/shell QDs seemed only to be nonblinking for the QDs with very thick shell, approximately >15 monolayers of CdS shell.[14,15,17] Based on this and their experimental results, Ghosh et al.[17] defined nonblinking volume threshold as 10% of dots with 99% of 'on' time. For wurtzite CdSe/CdS QDs, they further reported the nonblinking volume threshold was 750 nm^3. However, this value was found to be ~390 nm^3 by the Bawendi's group with their wurtzite CdSe/CdS QDs synthesized under substantially high reaction temperature (up to ~310 °C) and with long-time annealing after the epitaxial growth (~60 min).[18]

The phase-pure zinc-blende CdSe/CdS core/shell QDs studied here evidently differed from their wurtzite counterparts in terms of nonblinking volume threshold. Figures 6 and S5

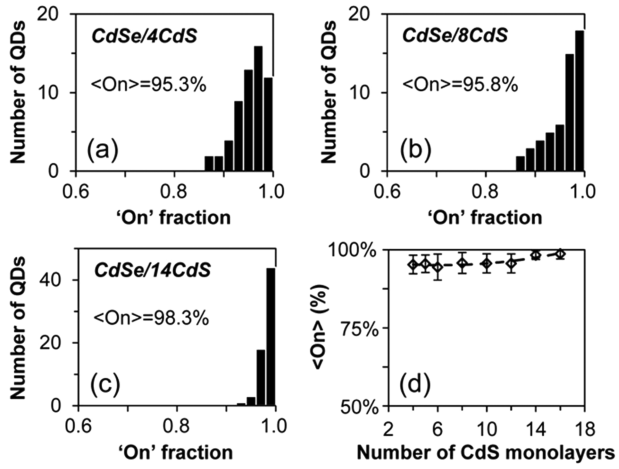

Figure 6. Statistical blinking properties of single CdSe/CdS QDs. (a–c) Histograms of the blinking 'on' time fraction for single zinc-blende CdSe/CdS core/shell QDs with 4, 8, and 14 monolayers of shell. (d) The average 'on' time fraction for single QDs with different number of CdS shell monolayers. More than 50 dots are randomly selected and measured for each QD sample.

revealed that, at a statistic level, the QDs with 4–16 monolayers of CdS shell were all nonblinking within single-exciton regime, with average 'on' time being ~95–99%. In Figure 6, even CdSe/4CdS (~100 nm^3 per dot) had about 20% dots with 99% of 'on' time. This means that, if there was a nonblinking volume threshold, it would be rather small—smaller than 100 nm^3—for the zinc-blende QDs.

It should be mentioned that the epitaxial growth temperature for the CdS shell for the entire series of QDs was not higher than 160 °C to avoid possible alloying and phase conversion from zinc-blende to wurtzite.[26] This temperature was significantly lower than that used in synthesis of any type of nonblinking core/shell QDs in literature. Therefore, the relatively small nonblinking volume threshold for wurtzite core/shell QDs reported by the Bawendi's group,[18] i.e., ~390 nm^3, should not be caused solely by their relatively high epitaxial temperature (up to ~310 °C).

Correlation of PL Spectra at Single-Dot and Ensemble Levels. The representative single-dot steady-state PL spectra for zinc-blende CdSe/CdS core/shell QDs with different shell thicknesses are shown in Figure 7a. For comparison, the

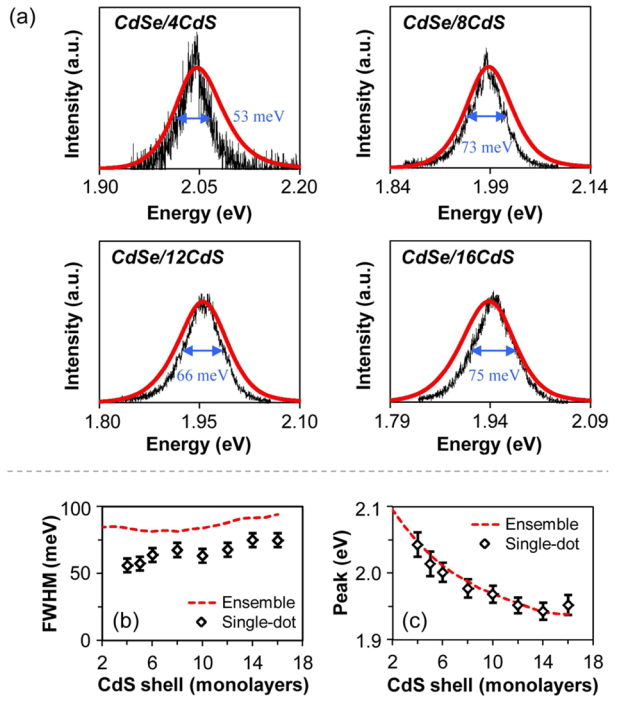

Figure 7. (a) Normalized steady-state PL spectra of single (black lines) and ensemble (red lines) zinc-blende CdSe/CdS core/shell QDs with 4, 8, 12, and 16 monolayers of shell. The fwhm of the PL spectra of single dots were labeled in blue. Shell-thickness-dependent PL fwhm and peak position of single and ensemble CdSe/CdS QDs with 4 to 16 monolayers of shell were summarized in (b) and (c).

corresponding PL spectrum recorded by an ensemble measurement was also plotted in Figure 7a for each case. The results in Figure 7 (Panel a) revealed that the single-dot PL spectra were always somewhat narrower than the corresponding ensemble ones. The peak width difference between single-dot and ensemble PL spectra was not as small as the best one recently reported by the Bawendi's group but it is approaching to the average level listed in their Supporting Information in the same report.[18]

Statistic data for multiple dot measurements on PL peak width at a single-dot level are illustrated in Figure 7b for further comparison. Statistically, the peak widths of single-dot PL spectra were only 17–33% narrower than those determined by ensemble measurements (Figure 7b). This first confirmed that the single-dot PL spectra shown in Figure 7a were representative for each sample. Second, each sample in the series was quite monodisperse in terms of PL spectra. To support the second claim, the statistic deviation of peak position of a single-dot spectrum measured for multiple dots from that of the corresponding ensemble PL was also summarized in Figure 7c. The results in Figure 7c revealed a very small deviation, <1%, for the entire series of QDs.

Overall, the results in Figure 7 revealed very good correlations between single-dot and ensemble PL spectra for

dx.doi.org/10.1021/ja4078528 | J. Am. Chem. Soc. 2014, 136, 179–187

a given sample, consistent with outstanding structural/optical quality of the samples at the ensemble level. In addition to what discussed above, the general trends of both peak shift (Figure 7c) and PL peak width evolution for the single-dot measurements (Figure 7b) followed similar trends for the corresponding ensemble measurement.

Unusual On/Off Probability Statistics. Kuno et al. and others[11,35−37] reported that the 'off' event probability of single QD blinking usually followed a strict power law and the 'on' event probability followed a truncated power law. Some variations from this type of typical power law statistics were also reported in literature. For example, the Bawendi's group reported that, instead of being truncated, the 'on' event probability also followed a strict power law.[18]

Figures 8 and S6 demonstrated a rather unique 'on' and 'off' event probability density distribution, which to our knowledge

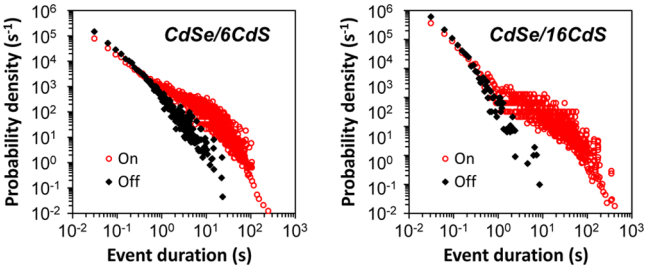

Figure 8. Log−log plot of the probability densities of 'on' and 'off' times for zinc-blende CdSe/CdS core/shell QDs with 6 and 16 monolayers of shell.

has not yet been reported in literature. The 'on' event probability of the phase-pure zinc-blende QDs showed an interesting 'expanded' power law at the long event duration tail, instead of a truncated power law. Conversely, the 'off' event probability was truncated at long 'off' time. Truncation of 'off' event probability power law implied that barely any long 'off' events occurred in the entire series of phase-pure zinc-blende QDs. At the same time, the probability densities of the long-term 'on' event (>1 s) were significantly above the power law tendency that the short-term 'on' events (<1 s) followed. These results indicated that this unique series of phase-pure zinc-blende CdSe/CdS core/shell dots possessed statistically more long 'on' events.

The truncation of 'off' probability and protrusion of 'on' probability from a power law, though unusual, was found to be consistent with the general feature of single-dot PL intensity time traces (Figures 2a and 4a,b), with long 'on' events isolated by occasional short 'off' events. This became more apparent if one observed the QDs with a long observation period (Figure 9). It should be pointed out that such blinking behaviors for this series of QDs could hold on for more than one day under continuous excitation with the same conditions.

One could put the interesting feature discussed above in a quantitative level. The results in Figures 8 and S6 revealed that the 'off' events longer than 1 sec were very rare in Figures 2a, 4a,b, and 9. For single-molecular tracking in cell, one second 'off' roughly corresponds to a diffusion distance smaller than 1 μm for biomolecule−QD complexes, which is approaching the resolution of optical microscope. In this sense, such QDs are practically 'nonblinking'.

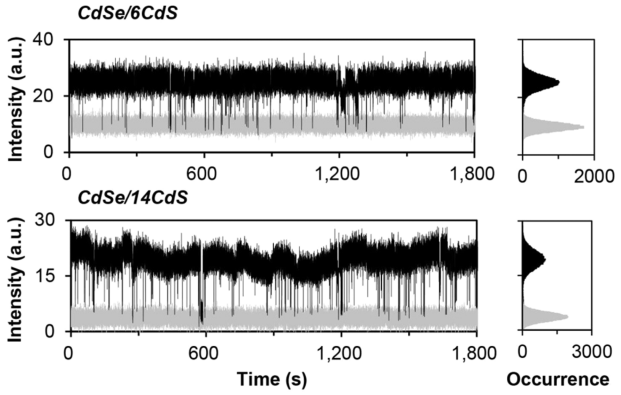

Figure 9. Representative offset-corrected PL intensity time traces (black) for 30 min of single zinc-blende CdSe/CdS core/shell QDs with 6 and 14 monolayers of shell and the corresponding histograms. The binning time is 30 ms. The background noise intensity time traces are in gray.

CONCLUSION

In summary, the first series of phase-pure CdSe/CdS core/shell QDs in zinc-blende structure was studied using single-dot spectroscopy. The single-dot spectroscopy studies were able to be carried out in single-exciton regime because of the outstanding structural perfection of the QDs, their extremely high PL QY—especially true for the thin-shell ones with relatively small absorption cross section and well-controlled excited-state properties. This enabled uncovering of the first series of core/shell QDs that are entirely nonblinking with their shell-thickness between 4 and 16 monolayers. In comparison with the reported results in literature, the zinc-blende CdSe/CdS core/shell QDs demonstrated rather different nonblinking volume threshold, 'on'/'off' probability density statistics, nonblinking intensity statistics (existence of unique '0−1' nonblinking behavior), and PL decay dynamics at both single-dot and ensemble levels. The well-controlled yet simple excited-state properties of this series of core/shell QDs should be the base of their outstanding properties at the single-dot level, which should play a key role in understanding the nature of blinking/nonblinking behaviors of QDs. Different from the results reported in literature, the thin- and medium-shell dots showed better single-dot optical properties than the thick-shell ones. This seemed to be consistent with the significantly better structural properties of the thin-shell QDs. The nonblinking and bright thin-shell QDs with much reduced sizes are of great interest for technical applications, such as being more permeable as biolabeling reagents.

EXPERIMENTAL SECTION

Sample Preparation, Morphological, and Structural Characterization. For a typical synthesis, the zinc-blende CdSe/CdS core/shell QDs with different shell thicknesses were synthesized using a new scheme developed on the basis of a reported one.[26] Briefly, the 3.1 nm zinc-blende CdSe core nanocrystals were synthesized[38] and purified[26] according to our recent reports. For CdS shell coating, dodecane (3.8 mL), octylamine (1.05 mL), oleylamine (0.45 mL), and purified CdSe core solution (containing about 2×10^{-7} mol of nanocrystals) were added to a three-neck flask under argon flow and then heated to 80 °C. For a reaction with 2×10^{-7} mol of 3.1 nm CdSe core, the amount for six consecutive injections of the $Cd(DDTC)_2$-amine solution was calibrated as 0.08, 0.12, 0.16, 0.21, 0.26, and 0.32 mL, respectively. When the first injection of $Cd(DDTC)_2$ precursor solution was injected into this reaction flask, the reaction solution was heated to 160

dx.doi.org/10.1021/ja4078528 | J. Am. Chem. Soc. 2014, 136, 179−187

°C in 5 min and kept for another 20 min. Then the reaction mixture was allowed to cool down to 80 °C, and the second injection of the $Cd(DDTC)_2$ precursor solution was applied. This reaction cycle, addition of the precursor solution at 80 °C and growth of CdS shell at a 150 °C for about 20 min for the optimal synthesis, was continued until six monolayers of CdS shell. From the seventh monolayer of CdS, precursor solutions (50% of $Cd(DDTC)_2$ and 50% of $Cd(Ol)_2$) in the calibrated volumes for each monolayer were injected, and the temperature was set at 160 °C. The calibrated volumes for growth of 7 to 16 monolayers of CdS shell were 0.39, 0.47, 0.55, 0.64, 0.73, 0.83, 0.94, 1.06, 1.19, and 1.31 mL, respectively, each of which included both $Cd(DDTC)_2$ and $Cd(Ol)_2$. The TEM images were taken on a Hitachi 7700 transmission electron microscope with an acceleration voltage of 80 kV using copper grids (400 mesh) coated with pure carbon support film. The XRD patterns were obtained using a Rigaku Ultimate-IV X-ray diffractometer operating at 40 kV/40 mA using Cu Kα line (λ = 1.5418 Å).

Optical Measurements on QDs in Ensemble Level. The PL and absorption spectra were measured using an Edinburgh Instruments FLS920 spectrometer and an Analytik Jena S600 UV−vis spectrophotometer, respectively. The absolute PL QY was measured using an Ocean Optics FOIS-1 integrating sphere coupled with a QE65000 spectrometer. Multiple measurements were performed with solutions in a series of optical densities for each QD sample. Time-resolved fluorescence spectra were measured via the time-correlated single-photon counting (TCSPC) method using an Edinburgh Instruments FLS920 fluorescence spectrometer with a 405 or 515 nm ps pulsed diode laser with 1 MHz repetition rate and ∼50 ps pulse duration.

Optical Measurements on QDs in Single-Dot Level. Samples for single QD measurements were prepared by spin-casting a dilute solution of zinc-blende CdSe/CdS core/shell QDs in a PMMA/toluene (0.5 wt %) onto a clean glass coverslip. All single-dot optical measurements were performed using a home-built epi-illumination fluorescence microscope system equipped with a Zeiss 63× oil immersion objective (numerical aperture = 1.46) and suitable spectral filters.

The excitation light source for PL intensity time traces, steady-state PL spectra, and second-order photon correlation measurements was a 405 nm continuous-wave laser. The excitation light source for the transient PL spectra for single dot was a 450 nm ps pulsed laser with 1 MHz repetition rate and 50 ps pulse duration.

There were two approaches performed in this report to monitor the blinking behavior of single dots. The PL intensity time traces of single dots were mostly recorded by an Andor DU-897 EMCCD. For PL intensity time trace measurements, movies with 30 ms exposure time per frame were recorded for designated time length. The emission intensity of each QD on each frame was determined by the mean of the gray values in a ∼1.4 × 1.4 μm^2 square containing the largest emission spot of the dot in all frames. The corresponding background intensity was determined by the mean of the gray values in a square of the same size closed to the QD but without any emission signal from visible QDs. Both the PL intensity and the background intensity were corrected by subtracting an average offset of EMCCD, which was measured without any input excitation laser. In particular, the PL intensity time traces in Figure 4 were recorded by a single-photon counting system (a PerkinElmer SPCM-AQRH-15-FC single-photon detectors and PicoQunat Picoharp 300 TCSPC electronics) in a time-tagged time-resolved mode. The former method could image and record the PL intensities of many single dots once. The latter one could simultaneously record the temporal PL intensities and PL decay dynamics for a single dot.

For steady-state PL spectra measurements in single-dot level, the PL signal from a single dot was collected by a multimode optical fiber and recorded by a Horiba Jobin Yvon iHR550 spectrometer. All spectra were collected for 20 s.

Second-order photon correlation measurements were performed with a Hanbury-Brown and Twiss (HBT) intensity correlation setup comprised of a 50/50 beam splitter, two PerkinElmer SPCM-AQRH-15-FC single-photon detectors, and PicoQunat Picoharp 300 TCSPC electronics.

■ ASSOCIATED CONTENT

Ⓢ Supporting Information

Additional table, figures, and movies. This material is available free of charge via the Internet at http://pubs.acs.org.

■ AUTHOR INFORMATION

Corresponding Authors

hattieqin@zju.edu.cn
wfang08@zju.edu.cn
xpeng@zju.edu.cn

Author Contributions

[§]These authors contributed equally.

Notes

The authors declare no competing financial interest.

■ ACKNOWLEDGMENTS

We are grateful for Prof. Limin Tong for the single-dot spectroscopy measurements. This work was supported in part by the National Basic Research Program of China (no. 2014CB921300), National Natural Science Foundation of China (NSFC, nos. 21233005, 21303159, 11104245, and J1210042), China Postdoctoral Science Foundation (CPSF, no. 2013M530281), and Fundamental Research Fund for the Central Universities (2013FZA3006).

■ REFERENCES

(1) Alivisatos, A. P. *Science* **1996**, *271*, 933.
(2) Nirmal, M.; Dabbousi, B. O.; Bawendi, M. G.; Macklin, J. J.; Trautman, J. K.; Harris, T. D.; Brus, L. E. *Nature* **1996**, *383*, 802.
(3) Colvin, V. L.; Schlamp, M. C.; Alivisatos, A. P. *Nature* **1994**, *370*, 354.
(4) Dahan, M.; Levi, S.; Luccardini, C.; Rostaing, P.; Riveau, B.; Triller, A. *Science* **2003**, *302*, 442.
(5) Michler, P.; Kiraz, A.; Becher, C.; Schoenfeld, W. V.; Petroff, P. M.; Zhang, L. D.; Hu, E.; Imamoglu, A. *Science* **2000**, *290*, 2282.
(6) Efros, A. L.; Rosen, M. *Phys. Rev. Lett.* **1997**, *78*, 1110.
(7) Krauss, T. D.; Brus, L. E. *Phys. Rev. Lett.* **1999**, *83*, 4840.
(8) Kuno, M.; Fromm, D. P.; Hamann, H. F.; Gallagher, A.; Nesbitt, D. J. *J. Chem. Phys.* **2001**, *115*, 1028.
(9) Schlegel, G.; Bohnenberger, J.; Potapova, I.; Mews, A. *Phys. Rev. Lett.* **2002**, *88*, 137401.
(10) van Sark, W. G. J. H. M.; Frederix, P. L. T. M.; Bol, A. A.; Gerritsen, H. C.; Meijerink, A. *ChemPhysChem* **2002**, *3*, 871.
(11) Frantsuzov, P.; Kuno, M.; Janko, B.; Marcus, R. A. *Nat. Phys.* **2008**, *4*, 519.
(12) Hohng, S.; Ha, T. *J. Am. Chem. Soc.* **2004**, *126*, 1324.
(13) Fomenko, V.; Nesbitt, D. J. *Nano Lett.* **2008**, *8*, 287.
(14) Chen, Y.; Vela, J.; Htoon, H.; Casson, J. L.; Werder, D. J.; Bussian, D. A.; Klimov, V. I.; Hollingsworth, J. A. *J. Am. Chem. Soc.* **2008**, *130*, 5026.
(15) Mahler, B.; Spinicelli, P.; Buil, S.; Quelin, X.; Hermier, J. P.; Dubertret, B. *Nat. Mater.* **2008**, *7*, 659.
(16) Wang, X. Y.; Ren, X. F.; Kahen, K.; Hahn, M. A.; Rajeswaran, M.; Maccagnano-Zacher, S.; Silcox, J.; Cragg, G. E.; Efros, A. L.; Krauss, T. D. *Nature* **2009**, *459*, 686.
(17) Ghosh, Y.; Mangum, B. D.; Casson, J. L.; Williams, D. J.; Htoon, H.; Hollingsworth, J. A. *J. Am. Chem. Soc.* **2012**, *134*, 9634.
(18) Chen, O.; Zhao, J.; Chauhan, V. P.; Cui, J.; Wong, C.; Harris, D. K.; Wei, H.; Han, H.-S.; Fukumura, D.; Jain, R. K.; Bawendi, M. G. *Nat. Mater.* **2013**, *12*, 445.
(19) Murray, C. B.; Kagan, C. R.; Bawendi, M. G. *Annu. Rev. Mater. Sci.* **2000**, *30*, 545.
(20) Peng, X. G. *Nano Res.* **2009**, *2*, 425.

(21) Fisher, B. R.; Eisler, H. J.; Stott, N. E.; Bawendi, M. G. *J. Phys. Chem. B* **2004**, *108*, 143.
(22) Spinicelli, P.; Buil, S.; Quelin, X.; Mahler, B.; Dubertret, B.; Hermier, J. P. *Phys. Rev. Lett.* **2009**, *102*, 136801.
(23) Galland, C.; Ghosh, Y.; Steinbruck, A.; Sykora, M.; Hollingsworth, J. A.; Klimov, V. I.; Htoon, H. *Nature* **2011**, *479*, 203.
(24) Galland, C.; Ghosh, Y.; Steinbruck, A.; Hollingsworth, J. A.; Htoon, H.; Klimov, V. I. *Nat. Commun.* **2012**, *3*, 908.
(25) Jin, S. Y.; Song, N. H.; Lian, T. Q. *ACS Nano* **2010**, *4*, 1545.
(26) Nan, W. N.; Niu, Y. A.; Qin, H. Y.; Cui, F.; Yang, Y.; Lai, R. C.; Lin, W. Z.; Peng, X. G. *J. Am. Chem. Soc.* **2012**, *134*, 19685.
(27) Efros, A. L.; Rosen, M.; Kuno, M.; Nirmal, M.; Norris, D. J.; Bawendi, M. *Phys. Rev. B* **1996**, *54*, 4843.
(28) Lakowicz, J. R. *Principles of Fluorescence Spectroscopy*; 3rd ed.; Springer: Baltimore, 2006.
(29) Michler, P.; Imamoglu, A.; Mason, M. D.; Carson, P. J.; Strouse, G. F.; Buratto, S. K. *Nature* **2000**, *406*, 968.
(30) Michler, P. *Single Quantum Dots: Fundamentals, Applications and New Concepts*; Springer: Berlin, 2003; Vol. *90*.
(31) Achermann, M.; Hollingsworth, J. A.; Klimov, V. I. *Phys. Rev. B* **2003**, *68*, 245302.
(32) Zhu, H. M.; Song, N. H.; Rodriguez-Cordoba, W.; Lian, T. Q. *J. Am. Chem. Soc.* **2012**, *134*, 4250.
(33) Brovelli, S.; Schaller, R. D.; Crooker, S. A.; Garcia-Santamaria, F.; Chen, Y.; Viswanatha, R.; Hollingsworth, J. A.; Htoon, H.; Klimov, V. I. *Nat. Commun.* **2011**, *2*, 280.
(34) Meijerink, A. In *Semiconductor Nanocrystal Quantum Dots: Sythesis, Assembly, Spectroscopy and Applications*; Rogach, A. L., Ed.; Springer: Vienna, 2008.
(35) Kuno, M.; Fromm, D. P.; Hamann, H. F.; Gallagher, A.; Nesbitt, D. J. *J. Chem. Phys.* **2000**, *112*, 3117.
(36) Shimizu, K. T.; Neuhauser, R. G.; Leatherdale, C. A.; Empedocles, S. A.; Woo, W. K.; Bawendi, M. G. *Phys. Rev. B* **2001**, *63*, 205316.
(37) Chung, I. H.; Bawendi, M. G. *Phys. Rev. B* **2004**, *70*, 165304.
(38) Pu, C. D.; Zhou, J. H.; Lai, R. C.; Niu, Y.; Nan, W. N.; Peng, X. G. *Nano Res.* **2013**, *6*, 652.